Potential energy curve for isomerization of N_2H_2 and C_2H_4 using the improved virtual orbital multireference Møller–Plesset perturbation theory

Rajat K. Chaudhuri,[1,a)] Karl F. Freed,[2,b)] Sudip Chattopadhyay,[3,c)] and Uttam Sinha Mahapatra[4,d)]

[1]*Indian Institute of Astrophysics, Bangalore 560 034, India*
[2]*The James Franck Institute and Department of Chemistry, University of Chicago, Chicago, Illinois 60637, USA*
[3]*Bengal Engineering and Science University, Shibpur, Howrah 711 103, India*
[4]*Department of Physics, Taki Government College, North 24 Parganas, Taki, India*

Multireference Møller–Plesset (MRMP) perturbation theory [K. Hirao, Chem. Phys. Lett. **190**, 374 (1992)] is modified to use improved virtual orbitals (IVOs) and is applied to study ground state potential energy curves for isomerization and dissociation of the N_2H_2 and C_2H_4 molecules. In contrast to traditional MRMP or *multistate* multiconfiguration quasidegenerate perturbation theory where the reference functions are obtained from (often difficult to converge) state averaged multiconfiguration self-consistent field methods, our reference functions are represented in terms of computationally efficient IVOs. For convenience in comparisons with other methods, a first order complete active space configuration interaction (CASCI) calculation with the IVOs is followed by the use of the IVOs in MRMP to incorporate residual electron correlation effects. The potential energy curves calculated from the IVO-MRMP method are compared with computations using state-of-the-art coupled cluster singles and doubles (CCSD) methods and variants thereof to assess the efficacy of the IVO-MRMP scheme. The present study clearly demonstrates that unlike the CCSD and its variants, the IVO-MRMP approach provides smooth and reliable ground state potential energy curves for isomerization of these systems. Although the rigorously size-extensive completely renormalized CC theory with noniterative triples corrections (CR-CC(2,3)) likewise provides relatively smooth curves, the CR-CC(2,3) calculations overestimate the *cis-trans* barrier height for N_2H_2. The ground state spectroscopic constants predicted by the IVO-CASCI method agree well with experiment and with other highly correlated *ab initio* methods. © *2008 American Institute of Physics*. [DOI: 10.1063/1.2837662]

I. INTRODUCTION

Despite tremendous methodological advances, an active current area of research involves the development of strategies capable of reliably computing global potential energy surfaces in a computationally cost effective fashion that maintains size-consistency over a vast spectrum of molecular geometries and that retains accuracy throughout the full potential energy surface. The great success of single reference (SR) formulations in describing systems that are predominantly of single determinantal character (so that correlation is primarily dynamical) has motivated numerous attempts to extend the limit of applicability of the SR approaches to bond breaking regions by treating the quasidegeneracy through the inclusion of the higher-body cluster operators associated with the quasidegenerate virtual orbitals. Consequently, low order perturbative approximations to SR approaches are incapable of providing a viable, accurate computational scheme in these quasidegenerate regions. On the other hand, the treatment of large systems with varying degree of quasidegeneracy and with actual or avoided curve crossings would greatly benefit from an accurate low order perturbation method.

Multireference (MR) generalizations of the SR theory describe the nondynamical electron correlation by using a reference space containing reference functions that can adequately describe the quasidegeneracy, while the dynamical electron correlation is introduced using MR-perturbation (MRPT) schemes. When applied to computing potential energy surfaces, however, some effective Hamiltonian based MRPT methods are often plagued by ubiquitous intruder problems,[1] thereby seriously limiting their viability for global surfaces. Among several recent attempts at devising a chemically accurate MRPT approach[2–8] for computing smooth potential surfaces, the most promising MRPT methods include those based on the use of a zeroth order multiconfiguration self-consistent field (MCSCF) or complex active space configuration interaction (CASCI) approximation, namely, the H^v,[2] MRMP,[3] multiconfiguration quasidegenerate perturbation theory (MCQDPT),[4] CASPT2,[5] multireference Møller–Plesset (MRMP) using APSG,[6] CIPSI,[7] etc., methods. The perturbation theory developed by Mukherjee and co-workers[8] (SS-MRPT) also has promising applicability for producing global potential energy surfaces.

a)Electronic mail: rkchaudh@iiap.res.in.
b)Electronic mail: freed@uchicago.edu.
c)Electronic mail: sudip_chattopadhyay@rediffmail.com.
d)Electronic mail: uttam.mahapatra@linuxmail.org.

The well-known rapid variation of orbitals upon traversing a curve crossing or avoided crossing in the computation of entire potential energy surfaces implies that it is crucial to construct the reference functions from orbitals that are optimal for describing the nondynamical correlation. Thus, a highly sophisticated MR many-body method is required, a realization motivating the recent development of various MR methods. The inclusion of dynamical correlation into mean field MR descriptions [say, MCSCF/complete active space self-consistent field (CASSCF)] of curve crossing regions shifts the crossing regions to completely different internuclear distances. Moreover, near the curve crossing zone, the determination of the orbitals and/or the geometry optimization with MCSCF/CASSCF approaches can encounter root flipping problems. While these difficulties can be mitigated using state average CASSCF (SA-CASSCF) approaches, these methods have drawbacks in (i) the difficulty in maintaining uniform quality for the states under consideration at all desired geometries; (ii) the problem of ensuring of orthogonality, which is important if, say, transition moments are to be computed; and (iii) the choice of weight factors used. [Item (iii) is a very laborious process since a plethora of numerical analysis is needed to obtain optimal weight factors.] The SA-CASSCF methods also exhibit considerable sensitivity in the convergence of the iteration scheme. Our applications instead generate the first order approximation with the improved virtual orbital (IVO)-CASCI technique that is free of these problems because the computations involve *no iterations* beyond an initial SCF approximation.

Although CASSCF/MCSCF methods are computationally simple and CASSCF energies are size extensive, some objections to these methods cite the fact that the dimension of the CAS grows very rapidly with an increase in the number of active orbitals. However, rather than striving for very large reference spaces, the initial CASSCF/MCSCF approximations are perturbatively corrected for correlation in MRPT approaches. Moreover, the ultimate growth in the size of the CAS in CASSCF/MCSCF schemes becomes limited by an increase in convergence difficulties which sometimes makes implementation of a MRPT computation impossible.[9] The convergence problems stem partially from the fact that the CASSCF procedure, in effect, attempts to optimize high lying states other than the ones of interest, and these higher states are poorly defined by the CAS employed. Moreover, the CASSCF treatments of properties other than energy differences, especially transition moments and oscillator strengths, are not very accurate.[10]

In 1993, Nakano[4] proposed a multistate version of quasidegenerate perturbation theory that begins with a MCSCF approximation (hence, the term MCQDPT) and that includes the MRMP variant of Hirao[3] as a subset. The MCQDPT reference functions are obtained using state averaged MCSCF methods which are susceptible to convergence difficulties (termed as intruder state effects) that render the MCQDPT approach computationally expensive, especially for a large CAS. To remove this objection, Nakano *et al.*[11] proposed using the quasicomplete active space (QCAS) SCF method, one of many multiconfiguration (MC) SCF approaches and a natural extension of the CASSCF method. In this scheme, the quasicomplete active space, which is a product of CAS spaces, serves as the variational space for the first order approximation. Note that the dimension of the QCAS can be much smaller than the CAS that is constructed from the same active orbitals and electrons.

Recently, we have proposed a computationally inexpensive version of MRMP/MCQDPT in which the first order reference functions are generated from the IVO-CASCI method[12–16] and then are used in subsequent MR perturbation calculations. The IVO-CASCI scheme is computationally simpler than CI-singles (CIS) and CASSCF methods. The latter arises because the IVO-CASCI calculations do not involve iterations beyond those in the initial SCF calculation, nor do they possess features that create convergence difficulties with increasing size of the CAS in CASCI calculations. Since the IVO-CASCI approach contains both singly and doubly excited configurations in the CAS (in addition to higher order excitations), it provides descriptions of both singly and doubly excited states with comparable accuracy to CASSCF treatments. The latter contrasts with the CIS method which cannot treat doubly excited states. Thus, the main computational advantages of our new developed IVO-MCQDPT approach over the traditional MCQDPT method are (i) the absence of iterations beyond those in the initial SCF calculation, and (ii) the lack of convergence difficulties from intruder states that plague CASSCF calculations with increasing size of the CAS.

The IVO-CASCI scheme differs from traditional CI and MP2 approaches in the evaluation of orbitals and orbital energies. The traditional CI and MP2 methods determine both the occupied and unoccupied orbitals and their orbital energies using a single Fock operator in which the unoccupied orbitals describe the motion of an electron in the field of N other electrons. Consequently, the virtual orbitals are, at best, more appropriate for describing negative ion states than the low lying excited states of interest. The IVO-CASCI method obtains the unoccupied orbitals and their energies from a V^{N-1} potential Fock operator in order to optimize the CASCI predictions for low lying electronic states and thereby to minimize the higher order perturbative corrections. The generation of improved virtual orbitals resembles the approach proposed long ago by Silverstone and Yin[17] and Huzinaga and Arnau[18] which is a special case of the extended Hartree–Fock method of Morokuma and Iwata.[19]

In the present Communication, we apply the IVO-CASCI version of MRMP to study the *cis-trans* reaction path of diimide (N_2H_2). The generation of a smooth and accurate potential energy curve of N_2H_2 along the *cis-trans* reaction path is a nontrivial problem as the character of the ground state reference function changes rapidly for a very small geometrical distortion. The ground states of *cis-* and *trans-*N_2H_2 are predominantly single reference in character, whereas they becomes highly multireference near the transition state geometry (for the dihedral angle $\alpha_d = 90°$). In addition, we also study cuts in the potential energy surface of C_2H_4 as a function of $H_2C–CH_2$ torsion angle. Like N_2H_2, the ground state of C_2H_4 also exhibits strong multireference character when the two CH_2 planes become perpendicular to each other. The ground state geometries of the *cis, trans,* and *iso* isomers are

determined using the IVO-CASCI optimization method and are compared both with experiment and with other treatments. The subsequent IVO-MRPT calculations provide the conformational energies and barrier heights, as well as curves for the *cis-trans* isomerization. The present work clearly demonstrates the IVO-CASCI version of MRMP method as a suitable alternative for providing accurate electronic structure calculations of complex molecular systems.

Section II provides a brief outline of the method for generating the improved virtual orbitals along with relevant equations describing the IVO scheme. The calculated results are presented and compared with other methods in the subsequent section.

II. GENERATION OF IMPROVED VIRTUAL ORBITALS (IVOs)

Before describing the generation of IVOs, it is pertinent to present the underlying philosophy behind their use. While the following arguments are applicable to arbitrary MC reference spaces, they are illustrated here for a CAS because the numerical computations proceed with a CAS reference space to facilitate comparisons with other methods.

Consider a calculation that uses a CAS specified by a set of doubly occupied core orbitals $\{c\}$ and a set of partially occupied valence orbitals $\{v\}$. The valence orbitals are further subdivided into those occupied $\{v_o\}$ in the reference state zeroth order wave function and those $\{v_u\}$ unoccupied in the reference state wave function. Otherwise, the orbitals are unspecified for now apart from symmetry types.

Let the dimension of the CAS be $D+1$, and partition the $D+1$ CAS functions into the reference state R and all others O_I, $I=1,\cdots D$. Further, assume that the O_I are chosen to diagonalize the Hamiltonian H in the $D\otimes D$ space of the other $\{O_I\}$, and designate their eigenvalues as E_I. With the aid of these definitions, Brillouin–Wigner perturbation theory for energy of the state R is given exactly in the CAS by

$$E_R = \langle R|H|R\rangle + \sum_{I=1}^{D} \frac{\langle R|H|O_I\rangle\langle O_I|H|R\rangle}{E - E_I}.$$

When R is an approximate ground state wave function, the variational principle implies that $E-E_I<0$, and, consequently, the contributions from each O_I are nonpositive. Since E_R is a upper bound to the ground state energy in the CAS, the best choice of orbitals is obtained from the set of orbitals $\{v_u\}$ that minimizes the E_I for the specified CAS. Clearly, there are three possible approaches, namely, (a) choose $\{v_u\}$ to minimize the denominators E_R-E_I, (b) choose $\{v_u\}$ to maximize the numerators, or (c) simultaneously optimize both.

The interleaving theorem[20] proves that the E_I are upper bounds to the eigenvalues of the $D\otimes D$ O_I space, so criterion (a) implies that the $\{v_u\}$ be chosen to give best approximate energies of *all the* excited CAS states. The use of Hartree–Fock (HF) orbitals for the $\{v_u\}$ clearly represents a poor choice in this regard since the HF orbitals $\{v_u\}$ are eigenfunctions of V^{N+1} potentials and are, at best, useful for describing the negative ion. HF orbitals also do not give best description of the excited states in the CAS. Using natural orbitals or

CASSCF orbitals for the R state represents an improvement over the HF orbitals, but these choices of the $\{v_u\}$ involve orbitals that are best suited for correlating the R state rather than describing the low lying excited states. The IVOs are specially defined to provide the best representation for the low lying excited states in the CAS that have the lowest energies (and thus lowest approximate E_I) and hence are likely to provide largest contribution to E_R. While improvements are definitely possible, especially for specific cases where certain O_I contribute most, the use of IVOs is clearly an improvement over the customary choices as far as the energy denominators are concerned.

One portion of the CASSCF procedure effectively involves a CASCI computation using orbitals optimized for a single state or for some weighted average of several states. A CI computation of dimension D is well known to provide rigorous upper bounds to the energies of the D lowest electronic states,[20] but, of course, accurate bounds are expected only for the lowest few of these states, which, fortunately, are generally the states of interest. However, the use of orbitals optimized for one (or for the average of a few) states generally yields a poor representation of the other states, and this feature is partially responsible for the poor convergence of the CASSCF procedure as the dimension of the CAS grows. Our alternative approach involves directly choosing orbitals that simultaneously provide a good representation for several of the lowest lying electronic states. This procedure is used in H^v computations, where the CAS orbitals are defined as comprising the highest occupied orbitals (perhaps, only for certain symmetries) in the SCF approximation to the ground (or a low lying) state and a set of the lowest lying IVO orbitals constructed from the remaining unoccupied space in the basis set. This approach is designed to maximize the accuracy of the first order H^v approximation, which is equivalent to a CASCI, for the low lying electronic states in order to minimize the required perturbative corrections.[21] Earlier H^v computations use a computationally complex sequence of SCF computations to obtain the IVOs, but more recently they employ a simple direct method for generating the IVOs for several common situations.[13] The significant improvement in computational efficiency for determining the IVOs is one important feature contributing to the package-ability of the IVO-CASCI method and its use for geometry optimization.[22] Indeed the IVO-CASCI programs have been made available for incorporation into GAMESS.

Since the basic philosophy of generating the IVOs is the same for both restricted and unrestricted HF orbitals, we only present the restricted HF case, which is used herein.

When the ground state of the system is a closed shell, we begin, for example, with the HF molecular orbitals (MOs) for the ground state wave function, $\Phi_0 = \mathcal{A}[\phi_1\bar{\phi}_1\phi_2\bar{\phi}_2\cdots\phi_n\bar{\phi}_n]$, where $\mathcal{A}$ is the antisymmetrizer and where the indices $i,j,k,\cdots$ refer to the occupied HF MOs $\{\phi_i\}$ and $u,v,w,\cdots$ to unoccupied HF MOs. All HF MOs are determined by diagonalizing the one-electron Hartree–Fock operator ^1F,

$$^1F_{lm} = \langle \phi_l | H + \sum_{k=1}^{\text{occ}} (2J_k - K_k) | \phi_m \rangle = \delta_{lm}\epsilon_l, \qquad (1)$$

where l and m designate any (occupied or unoccupied) HF MO and ϵ_l is the HF orbital energy. The operator H is the one-electron portion of the Hamiltonian, and J_k and K_k are Coulomb and exchange operators, respectively, for the occupied orbital ϕ_k. An excited state HF computation would provide a new set $\{\chi\}$ of MOs that produces the lowest possible energies for the low lying singly excited $\Psi_{\alpha \to \mu}$ state,

$$\Psi(\alpha \to \mu) = \mathcal{A}[\chi_1 \bar{\chi}_1 \chi_2 \bar{\chi}_2 \cdots (\chi_\alpha \bar{\chi}_\mu \pm \chi_\mu \bar{\chi}_\alpha) \cdots \chi_n \bar{\chi}_n], \qquad (2)$$

corresponding to excitation of an electron from the orbital χ_α to χ_μ, where the $+$ and $-$ signs correspond to triplet and singlet states, respectively. The new MOs $\{\chi_\alpha\}$ and $\{\chi_\mu\}$ may be expressed as a linear combination of the ground state MOs $\{\phi_i, \phi_u\}$. If, however, the orbitals are restricted such that the $\{\chi_\alpha\}$ are linear combinations of only the occupied ground state MOs $\{\phi_\alpha\}$ and the $\{\chi_\mu\}$ are expanded only in terms of the unoccupied $\{\phi_u\}$,

$$\chi_\alpha = \sum_{i=1}^{\text{occ}} a_{\alpha i} \phi_i, \quad \chi_\mu = \sum_{u=1}^{\text{unocc}} c_{\mu u} \phi_u, \qquad (3)$$

then the new orbital set $\{\chi_\alpha, \chi_\mu\}$ not only leaves the ground state wave function unchanged but also ensures orthogonality and the applicability of Brillouin's theorem for matrix elements between the HF ground state and the $\Psi_{\alpha \to \mu}$ excited states. In addition, this choice also benefits from using a common set of MOs for the ground and excited states, a choice that simplifies the computation of oscillator strengths, etc. However, we avoid the computationally laborious reoptimization of the occupied orbitals by setting $\{\chi_\alpha\} \equiv \{\phi_\alpha\}$, i.e., by choosing $a_{\alpha j} = \delta_{\alpha j}$, thereby enormously simplifying the procedure for generating the IVOs. Hence, the coupled equations determining the coefficients $a_{\alpha j}$ and $c_{\mu\nu}$ reduce to a single eigenvalue equation of the form $F'C = C\Gamma$, where the operator F' is given by

$$F'_{vw} = {}^1F_{vw} + A^\alpha_{vw}, \qquad (4)$$

where ^1F is the ground state Fock operator and where the additional term A^α_{vw} accounts for the excitation of an electron out of orbital ϕ_α,

$$A^\alpha_{vw} = \langle \chi_v | -J_\alpha + K_\alpha \pm K_\alpha | \chi_w \rangle. \qquad (5)$$

The minus sign in Eq. (5) applies for $^3\Psi_{\alpha \to \mu}$ a triplet state, while the plus sign is for the singlet $^1\Psi_{\alpha \to \mu}$ state.[18,23] The corresponding transition energy is

$$^{1,3}\Delta E(\alpha \to \mu) = E_0 + \gamma_\mu - {}^1F_{\alpha\alpha}, \qquad (6)$$

where E_0 is the HF ground state energy and γ_μ is the eigenvalue of $F'C = C\Gamma$ for the μth orbital.

Special care is required when the highest occupied HF MOs are doubly degenerate. In order that the $\{\chi_\mu\}$ retain molecular symmetry, the construction of F' must be modified from Huzinaga's scheme. If ϕ_α and ϕ_β are the highest
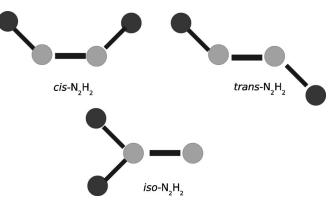

FIG. 1. Geometrical isomers of N_2H_2.

occupied degenerate HF MOs, then the matrix element A^α_{vw} in Eq. (6) is replaced for these degenerate systems by $A^{\alpha,\beta}_{vw}$, where

$$A^{\alpha,\beta}_{vw} = \tfrac{1}{2}\langle \chi_v | -J_\alpha + K_\alpha \pm K_\alpha | \chi_w \rangle$$
$$+ \tfrac{1}{2}\langle \chi_v | -J_\beta + K_\beta \pm K_\beta | \chi_w \rangle. \qquad (7)$$

While the IVOs may be applied to the MRPT method in conjunction with arbitrary reference spaces, the present computations employ a CAS to facilitate comparisons with other calculations of the geometries, conformational energy differences, barrier heights, dissociation energies, etc. Geometries are optimized with the IVO-CASCI optimization scheme, and the ground state IVO-CASCI wave function is used in evaluating the second order MRPT corrections. Third order H^v calculations also perform well, but the H^v treatment is more costly because it is designed for studying several states simultaneously, whereas the MRPT method is designed to focus on a single state at a time.

III. RESULTS AND DISCUSSION

A. N_2H_2

Trans-N_2H_2 (diazene, diimide) was produced by the decomposition of hydrazine[24] and hydrazoic acid[25] and was identified by mass spectrometry. Diazene/diimide is extensively used for stereospecific reductions of olefins[26] and as ligand for transition metal complexes.[27] N_2H_2 has also drawn considerable attention from theoretical chemists as accurate knowledge of its global potential energy surface is key to understanding the elementary reactions involved in the hydrogenation of nitrogen without the use of a catalyst.

Several studies have been devoted to determining the geometries, vibrational frequencies and the relative stabilities of the N_2H_2 isomers. While all published theoretical work unanimously agrees on the existence of three local minima, *trans*-, *cis*- and *iso*-N_2H_2 (depicted in Fig. 1), agreement for the transition states applies only for the transition state for conversion between the *cis-trans* isomers. The global potential surface/curve of N_2H_2 has been studied by Jensen *et al.*[28] using CASSCF calculations with a double-ζ basis set and by Hwang and Mebel[29] using second order Møller–Plesset (MP2) perturbation theory with a 6-31G** basis set. Most recently, Biczysko *et al.*[30] have optimized the geometries of all isomers with a MCSCF treatment using a full valence,

TABLE I. Geometrical parameters of the *trans*-N_2H_2 isomer. Bond lengths and bond angles are given in a.u and degrees, respectively.

Methods	CAS	Basis	R_{NN}	R_{NH}	$\angle HNN$
MCSCF[a]	$(12e, 10v)$	aug-cc-pVDZ	2.3897	1.9821	105.6
		aug-cc-pVTZ	2.3767	1.9702	105.9
		aug-cc-PVQZ	2.3741	1.9688	106.0
CASSCF	$(8e, 8v)$	aug-cc-pVDZ	2.3896	1.9731	105.8
		aug-cc-PVTZ	2.3764	1.9606	106.1
		aug-cc-PVQZ	2.3741	1.9591	106.2
		cc-pVQZ	2.3754	1.9590	106.1
	$(12e, 10v)$	aug-cc-pVDZ	2.3897	1.9821	105.6
		aug-cc-pVTZ	2.3764	1.9704	105.9
IVO-CASCI	$(8e, 8v)$	aug-cc-pVDZ	2.3523	1.9209	107.1
		aug-cc-pVTZ	2.3419	1.9080	107.3
		cc-pVQZ	2.3586	1.9184	106.4
	$(12e, 10v)$	aug-cc-pVDZ	2.3554	1.9327	106.9
		aug-cc-pVTZ	2.3400	1.9217	107.3
CCSD(T)[b]		cc-pVQZ	2.3561	1.9428	106.2
Expt.[c]			2.3565	1.9464	106.3

[a]Reference 30.
[b]Reference 32.
[c]Reference 41.

complete active space (with 12 active electrons and 10 active orbitals) as the reference function and the aug-cc-pVXZ (X =D,T,Q) basis sets of Dunning.[31] Biczysko *et al.*[30] have also performed a vibrational analysis to elucidate the nature of transition states. Since the main thrust of the present attempt is to delineate the efficacy of the IVO-MRMP method, we restrict considerations of basis set dependence to the determination of the geometrical parameters for the *trans*-, *cis*- and *iso*-N_2H_2 and the challenging problem of evaluating the potential energy curve for the *cis-trans* conversion of N_2H_2.

Table I compares the optimized geometrical parameters for *trans*-N_2H_2 from IVO-CASCI calculations using cc-pVQZ and aug-cc-pVXZ (X=D,T,Q) basis sets with those from other correlated calculations.[30,32] The IVO-CASCI geometry optimization is performed with eight active electrons distributed over eight active orbitals $(8e, 8v)$. The geometrical parameters from a $(12e, 12v)$ IVO-CASCI geometry optimization are also reported for selected basis sets to illustrate the dependence of bond lengths and the bond angle on the active space. The IVO-CASCI method is one portion of the latest generation of effective valence shell Hamiltonian computer codes that have been interfaced to the GAMESS program.[33] The CASSCF data are obtained using the DALTON package.[34]

Table I clearly reflect the well-known fact that the optimized geometrical parameters depend on the method and on the basis set used. The MCSCF, CASSCF, and IVO-CASCI optimized parameters also depend critically on the choice of the active space and/or number of active electrons used in the calculations. As can be seen from Table I, the optimized parameters obtained from the MCSCF calculations are reasonably close to the CASSCF optimized data, as anticipated since the MCSCF procedure is a subset of the CASSCF. Also apparent is an overall improvement in the MCSCF and

CASSCF calculated optimized geometries when proceeding from aug-cc-pVDZ to aug-cc-pVTZ basis sets. Further improvement of the basis set to aug-cc-pVQZ yields even better agreement with experiment. The average discrepancies in the MCSCF calculations for the bond lengths are $0.034a_0$, $0.022a_0$, and $0.021a_0$ for the aug-cc-pVDZ, aug-cc-pVTZ, and aug-cc-pVQZ basis sets, respectively, while the corresponding CASSCF deviations are $0.029a_0$, $0.017a_0$, and $0.015a_0$. The discrepancy in the MCSCF (CASSCF) predicted bond angle varies from 0.7° (0.3°) for aug-cc-pVDZ to 0.3° (1°) for the aug-cc-pVQZ basis. As can be seen from Table I, the $(8e, 8v)$ IVO-CASCI treatment fares better than the CASSCF calculation for the same *active space*. The average (absolute) deviations from experiment of the IVO-CASCI estimated bond lengths are $0.015a_0$, $0.026a_0$, and $0.021a_0$ for the aug-cc-pVDZ, aug-cc-pVTZ, and cc-pVQZ basis sets, respectively. The discrepancies in the bond lengths are reduced by $0.007a_0$ as we increase the CAS from $(8e, 8v)$ to $(12e, 10v)$.

Table II displays the ground state geometries of *cis*- and *iso*-N_2H_2, as determined from IVO-CASCI and other correlated calculations. Since the CCSD[T] estimated bond lengths and bond angle for the *trans*-isomer are quite accurate (off by $0.002a_0$) and our predicted geometry for these two isomers agrees favorably with the far more expensive CCSD[T] geometries, we believe that the IVO-CASCI geometry for *cis*- and *iso*-N_2H_2 should be in accord with the experiment.

Figure 2 displays the ground state energies of N_2H_2 computed as a function of HN–NH dihedral angle using the HF-MRMP (MRMP with HF orbitals), IVO-MRMP, CCSD,[35] and CR-CC(2,3) (Ref. 36) methods. The IVO-MRMP, CCSD, and CR-CC(2,3) energies are all determined using the aug-cc-pVTZ basis set and maintaining the experi-

TABLE II. Geometrical parameters of the *cis*- and *iso*-N_2H_2 isomers. Bond lengths and bond angles are given in a.u and degrees, respectively.

Methods	CAS	Basis	R_{NN}	R_{NH}	$\angle HNN$
cis-N_2H_2					
MCSCF[a]	$(12e,10v)$	aug-cc-pVDZ	2.3804	2.0006	111.5
		aug-cc-pVTZ	2.3732	1.9807	111.6
CASSCF	$(8e,8v)$	aug-cc-pVDZ	2.3935	1.9784	110.8
		aug-cc-pVTZ	2.3805	1.9662	111.0
	$(12e,10v)$	aug-cc-pVDZ	2.3865	1.9921	111.4
		aug-cc-pVTZ	2.3733	1.9810	111.7
IVO-CASCI	$(8e,8v)$	aug-cc-pVDZ	2.3545	1.9349	112.0
		aug-cc-pVTZ	2.3410	1.9234	112.3
	$(12e,10v)$	aug-cc-pVDZ	2.3562	1.9472	111.9
		aug-cc-pVTZ	2.3424	1.9347	112.1
CCSD(T)[b]		cc-pVQZ	2.3538	1.9523	111.9
iso-N_2H_2					
MCSCF[a]	$(12e,10v)$	aug-cc-pVDZ	2.3140	1.9973	124.1
		aug-cc-pVTZ	2.2291	1.9886	124.2
CASSCF	$(8e,8v)$	aug-cc-pVDZ	2.3234	1.9340	123.1
		aug-cc-pVTZ	2.3007	1.9276	123.3
	$(12e,10v)$	aug-cc-pVDZ	2.3140	1.9973	124.1
		aug-cc-pVTZ	2.2990	1.9886	124.2
IVO-CASCI	$(8e,8v)$	aug-cc-pVDZ	2.2955	1.9250	122.8
		aug-cc-pVTZ	2.2811	1.9164	122.9
	$(12e,10v)$	aug-cc-pVDZ	2.3160	1.9708	123.4
		aug-cc-pVTZ	2.2922	1.9582	123.5
CCSD(T)[b]		cc-pVQZ	2.3002	1.9544	123.5

[a]Reference 30.
[b]Reference 32.

mental bond lengths and bond angle of *trans*-N_2H_2 (see Table I) for various HN–NH dihedral angle ranging from 0° (*cis*) to 180° (*trans*). For clarity of comparison between methods, the IVO-CASCI, MRMP, IVO-MRMP, and CCSD ground state energies are shifted so that they all equal the CR-CC(2,3) energy at the *trans* geometry.

The N_2H_2 ground state wave function for the *cis*- and *trans*-equilibrium geometries (and nearby geometries) is predominantly single reference in character and can be represented by the configuration state functions (CSFs) $[(1-4)a^2(1-2)b^2]3b^24b^2$ and $[(1-3)a^2(1-3)b^2]4a^25a^2$ (in the C_2 point group), respectively. However, as the dihedral angle increases, the contribution of the doubly excited $[(1-4)a^2(1-2)b^2]3b^25a^2$ CSF increases and reaches a maximum at the transition state geometry (see Fig. 3). Note that the $[(1-4)a^2(1-2)b^2]3b^25a^2$ CSF is a doubly excited CSF with respect to both $[(1-4)a^2(1-2)b^2]3b^24b^2$ and $[(1-3)a^2(1-3)b^2]4a^25a^2$ configurations. Since the CCSD and CR-CC(2,3) approaches are single reference formulations, the generation of potential energy curves for the *cis* to *trans* conversion is expected to fail near the transition state geometry with these methods. The MRMP and IVO-MRMP methods, on the other hand, are not only capable of representing nondynamical electron correlation but also are very effective in treating states of mixed parentage. This explains

why only the IVO-MRMP calculation yields a smooth curve for the *cis* to *trans* conversion, while the curves from the IVO-CASCI, HF-MRMP, CCSD, and CR-CC(2,3) methods exhibit a *cusp* near the transition state.

The ground state dissociative potential energy curves of *trans*- and *iso*- are presented as a function N–N bond distance in Figs. 4 and 5, respectively. The *trans* isomer dissociates into two NH species, whereas *iso*-N_2H_2 dissociates into H_2N and N at large N–N distances. Since the *trans* isomer dissociates into two NH species, a CAS comprised of 12 electrons (omitting the $1s$ electrons of the nitrogen atom) and 10 orbitals ($2s$, $2p$ for nitrogen and $1s$ for hydrogen) is used to generate the ground state potential energy curves of *trans*- and *iso*-N_2H_2. The potential energy curves depicted in Figs. 4 and 5 clearly demonstrate the strength of the IVO-MRMP seheme. It is worth mentioning that CCSD [also CR-CC(2,3)] calculations diverge at large N–N distances for these two systems.

The accuracy of the IVO-MRMP energies may further be assessed by comparing their respective energies with those of the CR-CC(2,3) method for the *cis*- and *trans*-isomers because the CR-CC(2,3) approach offers highly reliable estimates of ground state energies for systems dominated by a single reference wavefunction. Table III and the associated potential energy curves in Figs. 2, 4, and 5 present
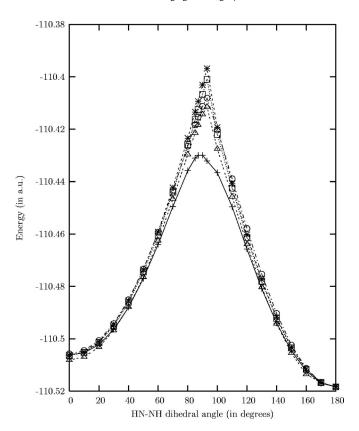
FIG. 2. The IVO-CASCI (○), IVO-MRMP (+), MRMP (△) CCSD (∗), and CR-CC(2,3) (□) ground state energies of N$_2$H$_2$ as a function of the HN–NH dihedral angle.

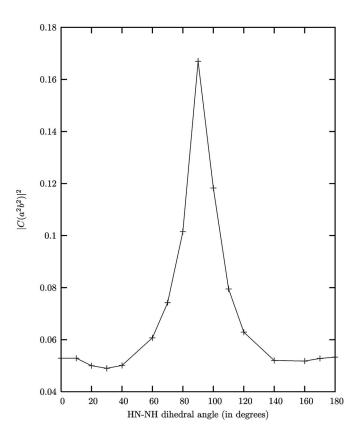FIG. 4. The IVO-MRMP ground state energy of *trans*-N$_2$H$_2$ as a function of N–N bond length.

FIG. 3. Contribution of doubly excited CSFs to the N$_2$H$_2$ ground state wave function as a function of HN–NH dihedral angle.

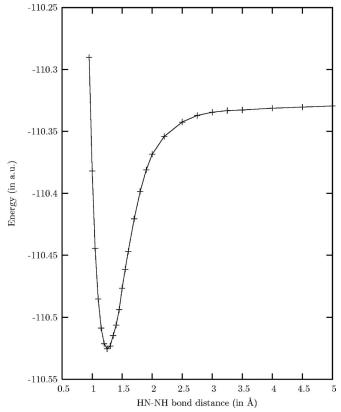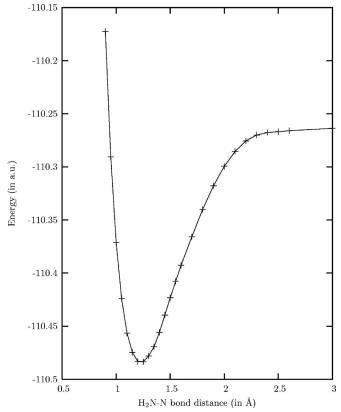
FIG. 5. The IVO-MRMP ground state energy of *iso*-N$_2$H$_2$ as a function of N–N bond length.

TABLE III. *trans-cis*, *trans-iso*, and *trans-TS* barrier height and zero point energy (ZPE) corrected bond fragmentation energy (in kcal/mol) of N_2H_2 isomers.

	IVO-MRMP[a]	CCSD[T][b]	MRCI[c]	MRCI+Q[c]	Experiment[d]
trans-	0.00	0.00	0.00	0.00	
cis-	5.87	5.21	5.03	5.05	
iso-	24.37	24.12	24.02	24.04	
TS	48.45		56.39	54.96	
NH+NH	115.32		119.00	118.88	121.6
NH_2+N	156.51		162.13	161.28	

[a]ZPE corrections (except for *trans*-TS) are estimated from experimental vibrational frequencies.
[b]Reference 32.
[c]Reference 30.
[d]Reference 29.

the *trans-cis*, *trans to transition state* barrier heights, as well as bond fragmentation energy of *trans*-N_2H_2 ($N_2H_2 \rightarrow$ NH +NH) and *iso*-N_2H_2 ($N_2H_2 \rightarrow H_2N$+N). Table III implies that the IVO-MRMP bond fragmentation energy departs only by 6 kcal/mol (off by 5%) from the multireference configuration interaction (MRCI) method and the experimental bond dissociation energy. The present calculation further exhibits the IVO-MRMP (CCSD) ground state energies as 4.49 (4.74) and 11.43 (11.31) kcal/mol, respectively, above the CR-CC(2,3) estimates for α_d=0° (180°). The agreement between the CC(2,3) and IVO-MRMP ground state energy (for α_d =0° and 180°) is, however, better for aug-cc-pVDZ basis. Our calculations show that IVO-MRMP (CCSD) ground state energies depart by 0.45 (0.03), 7.78 (7.72) kcal/mol, respectively, from the CR-CC(2,3) values for α_d=0° (180°). At this juncture, we emphasize that the computational time involved in the combined IVO-CASCI and IVO-MRMP calculations is an order of magnitude less than that required for CCSD and CR-CC(2,3) calculations.

B. C_2H_4

This subsection provides a study of the torsional potential energy curve of C_2H_4 (the rotation about C–C bond which leads the breaking of a π bond) to demonstrate that the IVO-MRMP can be employed to incorporate the important nondynamical electron effect efficiently. While this sinusoidal barrier is formally correct through first order in the wavefunction,[37] the presence of orbital degeneracy near the barrier top renders this computation a challenging test case for any MR theory.[38,39] An extensive list of earlier theoretical and experimental work for C_2H_4 is given in Ref. 40.

Twisted ethylene (at the D_{2d} geometry) is a generic example of a diradical transition state. Scrutiny of the MO model reveals that the p orbitals on carbon atoms lie perpendicular to the molecular plane and form bonding π and antibonding π^* orbitals at the equilibrium molecular geometry. As we twist the ethylene molecule around and about the C–C bond, the overlap between the two p orbitals decreases and finally vanishes near 90°. Therefore, at a torsional angle of 90°, the π and π^* orbitals become degenerate and the π-bond is completely ruptured. A $\pi \rightarrow \pi^*$ excitation in C_2H_4 provides a driving force for twisting around the C–C double bond and explains why *cis-trans* isomerization occurs in C_2H_4 (alkenes) upon $\pi \rightarrow \pi^*$ excitation. Therefore, a correct

description of ethylene near 90° demands the incorporation in the reference space of at least the the two configurations π^2 and π^*2. Numerical implementation indicates that the standard spin-restricted SR methods are unable to handle this degeneracy properly, and, therefore these SR treatments obtain an unphysical cusp in the torsional potential at 90°, i.e., at the top of the barrier. The potential energy curves generated from HF, SR CC, or CISD methods contain a pronounced cusp at 90° because the π^2 configuration is completely uncorrelated with the other important π^* configuration, whereas both configurations are important at the top of the barrier.[38] Thus a proper description of the torsional barrier of the ethylene mandates the use of a MR description.

Table IV compares the optimized geometrical parameters for C_2H_4, computed using the IVO-CASCI method, an $(8e, 8v)$ CAS, and the aug-cc-pVXZ (X=D,T) basis sets, with state-of-the-art CCSD treatments and with experiment. The IVO-CASCI optimized geometrical parameters for C_2H_4 exhibit a similar trend as that observed for the *trans*-N_2H_2 calculations, i.e., the accuracy of the geometrical parameters improves in proceeding from the aug-cc-pVDZ to aug-cc-pVTZ basis sets.

Figure 6 presents the ground state energies of C_2H_4, computed as a function of the H_2C–CH_2 dihedral angle using the IVO-MRMP, CCSD, and CR-CC(2,3) methods. The torsional potential is evaluated with all degrees of freedom frozen except for the torsional angle. The IVO-MRMP, CCSD, and CR-CC(2,3) calculations for H_2C–CH_2 employ the aug-cc-pVDZ basis set and are performed for variable dihedral angles from 0° to 180° with fixed values of R_{C-C} =1.339 Å, R_{C-H}=1.086 Å, and $\angle HCC$=117.6° (i.e., experimental ground state bond lengths and bond angles). For comparative purposes, the IVO-MRMP and CCSD ground state energies depicted in Fig. 6 are shifted such that they all equal the CR-CC(2,3) energy for the planar dihedral angle α_d=0°. Figure 6 demonstrates that only the IVO-MRMP calculation yields a smooth curve, whereas the CCSD and CR-CC(2,3) exhibit a cusp for α_d=90° because near the twisted region, the ground state wavefunction is multireference in character and cannot be described accurately with a single reference theory like CCSD and/or its variants.

IV. CONCLUDING REMARKS

We have investigated the torsional potential energy curve of N_2H_2 using the improved virtual orbital complete

TABLE IV. Geometrical parameters for C_2H_4. Bond lengths and bond angles are in Å and degrees, respectively.

Methods	CAS	Basis set	R_{CC}	R_{CH}	∠HCH
IVO-CASCI	$(8e, 8v)$	cc-pVDZ	1.340	1.088	116.6
		pVTZ	1.333	1.077	116.6
		aug-cc-pVDZ	1.323	1.083	116.8
		aug-cc-pVTZ	1.314	1.076	116.6
	$(12e, 12v)$	aug-cc-pVDZ	1.344	1.086	117.0
		aug-cc-pVTZ	1.335	1.078	116.9
CCSD		cc-pVDZ	1.345	1.096	116.9
		cc-pVTZ	1.327	1.077	117.1
		aug-cc-pVDZ	1.348	1.094	116.9
		aug-cc-pVTZ	1.327	1.078	117.1
Experiment[a]			1.339	1.086	117.6

[a]Reference 42.

active space configuration interaction (IVO-CASCI) version of multireference Møller–Plesset (MRMP) perturbation theory with aug-cc-pVXZ (X=D,T,Q) basis sets. Previous papers[16,22] have shown that geometries and bond fragmentation energies calculated with the IVO-CASCI/IVO-MRMP method agree well with experiment and with other correlated calculations. The present calculations further demonstrate that unlike the CCSD and/or CR-CC(2,3) approaches, the IVO-MRMP method is capable of producing smooth potential energy curve for *cis-trans* conversions since a similar trend is observed for the isomerization of the C_2H_4 molecule. We further emphasize that IVO-CASCI and IVO-MRMP methods are highly cost effective compared to the CCSD
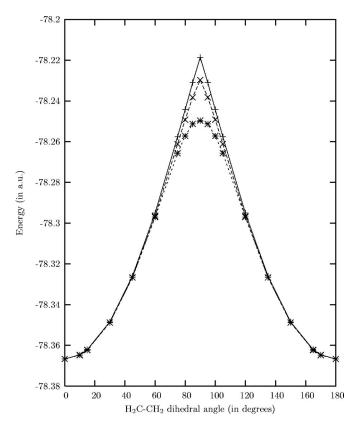
treatment and its variants. Moreover, the IVO-CASCI method does not require tedious and costly iterations beyond those in the initial SCF calculation, nor does it possess features that create convergence difficulties with increasing size of the CAS in CASCI calculations. This feature adds an additional advantage to IVO-MRMP calculations over those of the traditional MRMP which often encounters convergence difficulties within the MCSCF procedure. Since the IVO-MRMP approach does not use state averaged reference functions, the computation of transition dipole matrix elements between the states is trivial.

The numerical gradient formulation of the IVO-CASCI geometry optimization scheme is used to determine the structural parameters. A vibrational analysis is not presented because of the computational cost with numerical gradients, especially for polyatomic systems. The code for implementing the analytic gradient formulation of IVO-CASCI geometry optimization is currently under development and will be better suited for evaluating the frequencies.

FIG. 6. The IVO-MRMP (∗), CCSD (+), and CR-CC(2,3) (×) ground state energies of C_2H_4 as a function of $H_2C–CH_2$ dihedral angle.

[1] T. H. Schucan and H. A. Weidenmüller, Ann. Phys. **73**, 108 (1972).
[2] K. F. Freed, in *Lecture Notes in Chemistry*, edited by U. Kaldor (Springer-Verlag, Berlin, 1989), Vol. 52.
[3] K. Hirao, Int. J. Quantum Chem. **S26**, 517 (1992); Chem. Phys. Lett. **201**, 59 (1993).
[4] H. Nakano, J. Chem. Phys. **99**, 7983 (1993).
[5] K. Andersson, P. Å. Malmqvist, B. O. Roos, A. J. Sadlej, and K. Wolinski, J. Phys. Chem. **94**, 5483 (1990); K. Andersson, P. Å. Malmqvist, and B. O. Roos, J. Chem. Phys. **96**, 1218 (1992).
[6] E. Rosta and P. R. Surján, J. Chem. Phys. **116**, 878 (2002); P. R. Surján, Z. Rolik, Á. Szabados, and D. Kőhalmi, Ann. Phys. **13**, 223 (2004).
[7] B. Huron, J. P. Malrieu, and P. Rancurel, J. Chem. Phys. **58**, 5745 (1973); R. Cimiraglia, *ibid.* **83**, 1746 (1985).
[8] U. S. Mahapatra, B. Datta, and D. Mukherjee, J. Phys. Chem. A **103**, 1822 (1999); P. Ghosh, S. Chattopadhyay, D. Jana, and D. Mukherjee, Int. J. Mol. Sci. **3**, 733 (2002).
[9] A. Honing, M. Mandel, M. L. Stitch, and C. H. Townes, Phys. Rev. **96**, 629 (1954); K. P. Huber and G. Herzberg, *Milecular Spectra and Mo-*

lecular Structure (Van Nostrand Reinhold, NY, 1979), Vol. 4; D. L. Cooper, S. Bienstock, and A. Dalgarno, J. Chem. Phys. **86**, 3845 (1987); T. Pluta, Mol. Phys. **99**, 1535 (2001); P. F. Weck, K. Kirby, and P. C. Stancil, J. Chem. Phys. **120**, 4216 (2004).

[10] B. O. Roos, in *Advances in Chemical Physics*, edited by K. P. Lawley (Wiley Interscience, New York, 1987), Vol. 69, p. 339.

[11] H. Nakano, J. Nakatini, and K. Hirao, J. Chem. Phys. **114**, 1133 (2001).

[12] D. M. Potts, C. M. Taylor, R. K. Chaudhuri, and K. F. Freed, J. Chem. Phys. **114**, 2592 (2001).

[13] R. K. Chaudhuri, K. F. Freed, and D. M. Potts, in *Low Lying Potential Energy Surfaces*, edited by M. R. Hoffman and K. G. Dyall (Oxford University Press, Oxford, 2002), Ser. 828, p. 154; R. K. Chaudhuri, K. F. Freed, S. A. Abrash, and D. M. Potts, J. Mol. Struct.: THEOCHEM **83**, 547 (2001).

[14] C. M. Taylor, R. K. Chaudhuri, and K. F. Freed, J. Chem. Phys. **122**, 044317 (2005).

[15] R. K. Chaudhuri and K. F. Freed, J. Chem. Phys. **122**, 204111 (2005) and references therein.

[16] S. K. Chattopadhyay, U. S. Mahapatra, and R. K. Chaudhuri, Indian J. Phys. (in press).

[17] H. Silverstone and M. L. Yin, J. Chem. Phys. **49**, 2026 (1968).

[18] S. Huzinaga and C. Arnau, Phys. Rev. A **1**, 1285 (1970); J. Chem. Phys. **54**, 1948 (1971); D. McWilliams and S. Huzinaga, *ibid.* **55**, 2604 (1971).

[19] K. Morokuma and S. Iwata, Chem. Phys. Lett. **16**, 192 (1972).

[20] J. K. L. MacDonald, Phys. Rev. **43**, 830 (1933).

[21] J. E. Stevens, R. K. Chaudhuri, and K. F. Freed, J. Chem. Phys. **105**, 8754 (1996).

[22] R. K. Chaudhuri and K. F. Freed, J. Chem. Phys. **126**, 114103 (2007).

[23] J. P. Finley and K. F. Freed, J. Chem. Phys. **102**, 1306 (1995).

[24] S. N. Foner and R. L. Hudson, J. Chem. Phys. **28**, 719 (1958).

[25] E. D. Becker, G. C. Pimentel, and M. Van Thiel, J. Chem. Phys. **26**, 145 (1957); M. van Thiel and G. C. Pimentel, *ibid.* **32**, 133 (1960); K. Rosengren and G. C. Pimentel, *ibid.* **43**, 507 (1965).

[26] W. J. Noble, *Highlights of Organic Chemistry* (Dekker, New York, 1974); S. K. Vidyarthu, C. Willis, R. A. Back, and R. M. McKittrick, J. Am. Chem. Soc. **96**, 7647 (1974).

[27] M. Veith, Angew. Chem., Int. Ed. Engl. **15**, 387 (1976).

[28] H. J. A. Jensen, P. Jorgensen, and T. Helgaker, J. Am. Chem. Soc. **109**, 2895 (1987).

[29] D. Y. Hwang and A. M. Mebel, J. Phys. Chem. A **107**, 2865 (2003).

[30] M. Biczysko, L. A. Poveda, and A. J. C. Varandas, Chem. Phys. Lett. **424**, 46 (2006).

[31] T. H. Dunning, Jr., J. Chem. Phys. **90**, 1007 (1989); D. E. Woon and T. H. Dunning, Jr., *ibid.* **98**, 1358 (1993).

[32] J. M. L. Martin and P. R. Taylor, Mol. Phys. **96**, 681 (1999).

[33] M. W. Schmidt, K. K. Baldridge, J. A. Boatz, S. T. Elbert, M. S. Gordon, J. H. Jensen, S. Koseki, N. Matsunaga, K. A. Nguyen, S. J. Su, T. L. Windus, M. Dupuis, and J. A. Montgomery (unpublished).

[34] Release 1.2(2001), written by T. Helgaker, H. J. Aa. Jensen, P. Joergensen, J. Olsen, K. Ruud, H. Aagren, A. A. Auer, K. L. Bak, V. Bakken, O. Christiansen, S. Coriani, P. Dahle, E. K. Dalskov, T. Enevoldsen, B. Fernandez, C. Haettig, K. Hald, A. Halkier, H. Heiberg, H. Hettema, D. Jonsson, S. Kirpekar, R. Kobayashi, H. Koch, K. V. Mikkelsen, P. Norman, M. J. Packer, T. B. Pedersen, T. A. Ruden, A. Sanchez, T. Saue, S. P. A. Sauer, B. Schimmelpfennig, K. O. Sylvester-Hvid, P. R. Taylor, and O. Vahtras, RELEASE 1.2 (2002).

[35] F. Coester, Nucl. Phys. **7**, 421 (1958); F. Coester and H. Kümmel, *ibid.* **17**, 477 (1960); J. Čížek, J. Chem. Phys. **45**, 4256 (1966); Adv. Chem. Phys. **14**, 35 (1969); J. Čížek and J. Paldus, *ibid.* **9**, 105 (1975); R. J. Bartlett and W. D. Silver, Int. J. Quantum Chem. **S9**, 183 (1975); R. J. Bartlett, Annu. Rev. Phys. Chem. **32**, 359 (1981); J. Phys. Chem. **93**, 1697 (1989); *Modern Electronic Structure Theory*, edited by D. R. Yarkony (World Scientific, Singapore, 1995).

[36] P. Piecuch, S. A. Kucharski, K. Kowalski, and M. Musia, Comput. Phys. Commun. **149**, 71 (2002); P. Piecuch and M. Wloch, J. Chem. Phys. **123**, 224105 (2005).

[37] K. F. Freed, Chem. Phys. Lett. **2**, 255 (1968).

[38] A. I. Krylov, C. D. Sherill, E. F. C. Byrd, and M. Head-Gordon, J. Chem. Phys. **109**, 10669 (1998); A. I. Krylov and C. D. Sherill, *ibid.* **116**, 3194 (2002); J. S. Sears, C. D. Sherill, and A. I. Krylov, *ibid.* **118**, 9084 (2003).

[39] M. L. Abrams and C. D. Sherrill, Chem. Phys. Lett. **395**, 227 (2004).

[40] R. K. Chaudhuri, A. Mudholkar, K. F. Freed, C. H. Martin, and H. Sun, J. Chem. Phys. **106**, 9252 (1997).

[41] J. Damaison, F. Hegelund, and H. Burger, J. Mol. Struct. **413–414**, 447 (1997).

[42] G. Herzberg, *Electronic Spectra and Electronic Structure of Polyatomic Molecules* (Von Nostrand Reinhold, New York, 1966).